

Alma Mater Studiorum Università di Bologna
Archivio istituzionale della ricerca

Dielectric spectroscopy as a condition monitoring technique for cable insulation based on crosslinked polyethylene

This is the final peer-reviewed author's accepted manuscript (postprint) of the following publication:

Published Version:

Linde, E., Verardi, L., Fabiani, D., Gedde, U.W. (2015). Dielectric spectroscopy as a condition monitoring technique for cable insulation based on crosslinked polyethylene. POLYMER TESTING, 44, 135-142 [10.1016/j.polymertesting.2015.04.004].

Availability:

This version is available at: <https://hdl.handle.net/11585/554963> since: 2016-07-18

Published:

DOI: <http://doi.org/10.1016/j.polymertesting.2015.04.004>

Terms of use:

Some rights reserved. The terms and conditions for the reuse of this version of the manuscript are specified in the publishing policy. For all terms of use and more information see the publisher's website.

This item was downloaded from IRIS Università di Bologna (<https://cris.unibo.it/>).
When citing, please refer to the published version.

(Article begins on next page)

This is the final peer-reviewed accepted manuscript of:

E. Linde, L. Verardi, D. Fabiani, U.W. Gedde,

Dielectric spectroscopy as a condition monitoring technique for cable insulation based on crosslinked polyethylene

In:

Polymer Testing, Volume 44, 2015, Pages 135-142

The final published version is available online at:

<https://doi.org/10.1016/j.polymertesting.2015.04.004>

Rights / License:

The terms and conditions for the reuse of this version of the manuscript are specified in the publishing policy. For all terms of use and more information see the publisher's website.

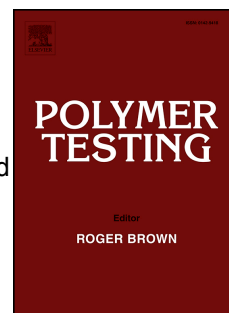
This item was downloaded from IRIS Università di Bologna (<https://cris.unibo.it/>)

When citing, please refer to the published version.

Accepted Manuscript

Dielectric spectroscopy as a condition monitoring technique for cable insulation based on crosslinked polyethylene

E. Linde, L. Verardi, D. Fabiani, U.W. Gedde



PII: S0142-9418(15)00094-X

DOI: [10.1016/j.polymertesting.2015.04.004](https://doi.org/10.1016/j.polymertesting.2015.04.004)

Reference: POTE 4420

To appear in: *Polymer Testing*

Received Date: 27 February 2015

Accepted Date: 8 April 2015

Please cite this article as: E. Linde, L. Verardi, D. Fabiani, U.W. Gedde, Dielectric spectroscopy as a condition monitoring technique for cable insulation based on crosslinked polyethylene, *Polymer Testing* (2015), doi: 10.1016/j.polymertesting.2015.04.004.

This is a PDF file of an unedited manuscript that has been accepted for publication. As a service to our customers we are providing this early version of the manuscript. The manuscript will undergo copyediting, typesetting, and review of the resulting proof before it is published in its final form. Please note that during the production process errors may be discovered which could affect the content, and all legal disclaimers that apply to the journal pertain.

Test Method

Dielectric spectroscopy as a condition monitoring technique for cable insulation based on crosslinked polyethylene

E. Linde^a, L. Verardi^b, D. Fabiani^b, U. W. Gedde^{a,*}

^a *KTH Royal Institute of Technology, School of Chemical Science and Engineering,
Fibre and Polymer Technology, SE-100 44 Stockholm, Sweden*

^b *Laboratory of Innovation Technology, Dept. of Electrical, Electronic and Information
Engineering, University of Bologna, Italy*

* Corresponding author. E-mail: gedde@kth.se
Phone: +46 8 790 7640. Fax: +46 8 208856.

ABSTRACT

Dielectric spectroscopy was evaluated as a condition monitoring technique for aged polyethylene electrical insulation in nuclear power plants. Bare core insulations of crosslinked polyethylene were aged at 55 and 85 °C under exposure to ^{60}Co γ -radiation at different dose rates (0.42, 0.76 and 1.06 kGy h⁻¹) to different total doses. The samples were studied by dielectric spectroscopy and tensile testing, and the crystallinity, mass fraction of soluble component and density were determined. The oxidation profiles along the depth of the insulations were assessed by infrared microscopy. The aged samples showed an increase in both the real and imaginary parts of the dielectric permittivity over the whole frequency range studied, an increase in the mass fraction of soluble component and in the material density, and a decrease in the strain-at-break. The imaginary part of the dielectric permittivity at 100 kHz increased in a linear fashion with increasing material density, the latter being strictly related to the extent of oxidation of the material according to infrared spectroscopy and differential scanning calorimetry. The generic relationship between the imaginary part of the permittivity and the density included all the data obtained under different ageing conditions. The results suggest that dielectric spectroscopy can be used for *in-situ* measurements of the degree of oxidation of polyethylene cables, in order to obtain information about the condition of the cable insulation to enable the remaining lifetime to be predicted.

Keywords:

Polyethylene

Radiation ageing

Thermal ageing

Dielectric response

Density

Condition monitoring

1. Introduction

For the safe and reliable operation of nuclear power plants, all significant components have to fulfil their function over their whole lifetime. This includes a wide range of polymeric materials used in, for example, cable insulation, seals and membranes. There are hundreds of kilometres of low-voltage instrumentation and control cables in a typical nuclear power plant, and their functionality relies on the condition of the polymeric insulation so that it is possible to transmit a signal without disturbance or the risk of a short circuit. The operating environment in a nuclear power plant, with elevated temperatures and with γ -radiation in some instances, causes irreversible changes to the chemical and physical structures of the polymeric materials, and thereby also to their vital functional properties [1–3]. For many polymers, including crosslinked polyethylene, these changes are caused by oxidation [4].

A component that affects the safety needs to undergo a qualification process in order to confirm that the intended function can be fulfilled throughout its intended lifetime. The long expected lifetimes, often spanning over several decades, necessitate accelerated ageing tests at elevated temperatures and high irradiation dose rates. After ageing of the samples, tests to evaluate the condition of the aged specimen have to be performed. The results of accelerated thermal ageing can be extrapolated to service temperatures using e.g. the Arrhenius law, and to different dose rates by considering the total absorbed dose. However, during accelerated ageing, it is important that the mode and rate-limiting factor remains the same over the extrapolation region [2,5,6]. At excessively high temperatures or high dose rates, the rate of diffusion of oxygen can limit the ageing, e.g. if the rate of consumption of oxygen is faster than the rate of resupply of oxygen by diffusion [7,8]. Diffusion-limited oxidation (DLO) has to be considered in the analysis of aged samples and also in the extrapolation of data taken on samples with non-homogeneous oxidation. Surface-sensitive measurements such as indentation modulus measurements show a close relationship with the strain-at-break; cracks are initiated in the degraded surface layer.

An important result of ageing is the embrittlement of the cable insulation. Mechanical testing, primarily the assessment of the strain-at-break, is commonly used to assess the condition of the insulation [9]. A critical strain-at-break of 50 % is one of the commonly used failure criteria, often in combination with criteria based on the functional properties of safety-related cables [2]. Tensile testing is a destructive method that consumes relatively large amounts of sample. This motivates the use of other test methods that use only small amounts of sample, e.g. measurements of density [10,11], oxidation induction time [12–14], oxygen

consumption [15], soluble fraction [16,17] and degree of oxidation by infrared spectroscopy [13,18]. However, even these methods are destructive and require sample removal.

For the non-destructive testing of already installed cables, several electrical techniques have been proposed, such as line resonance analysis (LIRA) [19], measurements of voltage return [20] and dielectric loss factor [21]. This paper deals with dielectric spectroscopy, which has a proven potential for the condition monitoring of cables insulated with EPR and EPDM rubbers [22–25], crosslinked polyethylene [26] and chlorosulphonated polyethylene [27]. Dielectric spectroscopy has been used as a tool to detect water trees in insulation of medium- and high-voltage cables [28–30]. The aim of the present work is to further explore the possibility of using dielectric spectroscopy as a non-destructive and online condition monitoring technique for crosslinked polyethylene cable insulations used in low-voltage cables in nuclear power plants.

2. Experimental

2.1. Materials

Crosslinked polyethylene insulation obtained from an Alcatel RG-59 B cable was studied. The EVA jacketing and copper/polyester screens were removed before ageing, so that only the insulation and the single copper strand (diameter = 0.6 mm) conductor remained. The wall thickness of the insulation was 1.6 mm. It consisted of colourless, peroxide-crosslinked polyethylene, with a density of 917 kg m^{-3} . Thermogravimetric analysis revealed that the polymer contained ca. 1 wt.% ash after heating in nitrogen to 600°C and then further to 1000°C in oxygen.

2.2. Accelerated ageing

Cable insulation samples, 10 m long, were aged at five different temperature/dose rate combinations at the ROZA facility at ÚJV Řež, a. s., Czech Republic, after the jacketing had been removed. The ageing was performed under both elevated temperature and γ -radiation from a ^{60}Co γ -ray source. The combinations of ageing temperature and dose rate used were: 55°C at 0.76 and 1.06 kGy h^{-1} , and 85°C at 0.42, 0.76 and 1.06 kGy h^{-1} . The dose rates used were sufficiently high to expect some diffusion-limiting effects [31]. The maximum ageing time under each condition was 1000 h. Specimens were removed for analysis every 200 h.

2.3. Dielectric spectroscopy

Dielectric spectroscopy was performed using a Novocontrol Alpha Dielectric Analyzer V2.2 operating between 10^{-2} and 10^6 Hz. The applied voltage was $3 V_{\text{rms}}$ and the test temperature was $50\text{ }^{\circ}\text{C}$. The cable samples were assessed by applying the input voltage to the central metal conductor and measuring the output signal from a wire braid placed on the outer surface of the insulation.

2.4. Determination of density

The density of aged and unaged specimens was determined using the Archimedes principle, weighing each specimen in both air and ethanol (96 vol.% ethanol, 4 vol.% water) on a Precisa XR 205SM-DR microbalance. Three replicates for each sample were used. The specimens were cut from the entire cross-section of the insulation.

2.5. Determination of mass fraction of soluble component

Three samples, weighing 450 ± 75 mg, of unaged samples and samples aged for 200, 600 and 1000 h at each combination of temperature and dose rate were cut from the whole cross-section of the cables and reflux-boiled in xylene (CAS No. 1330-20-7; $\geq 98\%$ purity; VWR Prolabo) for 8 h. The samples were then dried in a ventilated oven (Mettler ULE-600) at $50\text{ }^{\circ}\text{C}$ for 12 h, and the dry mass of the samples was obtained using a Precisa XR 205SM-DR microbalance. The mass fraction of soluble component in the polymer was calculated as the mass difference relative to the initial mass of the samples. The process was then repeated on the same samples in order to ensure complete extraction, and the difference in sample mass between first and second run was only ca. 1 %.

2.6. Tensile testing

Tubular insulation specimens (length ≥ 60 mm) were prepared from unaged and aged cable samples by removing the internal copper conductor. The stress-strain properties of these samples (initial gauge length = 20 mm) were assessed at $23 \pm 1\text{ }^{\circ}\text{C}$ and 50 %RH in an Instron 5566 Universal Testing Machine, using an extension rate of 12.5 mm min^{-1} . Six replicates were tested for each sample.

2.7. Infrared microscopy

The degree of oxidation at different depths in the insulation samples was determined using a Perkin-Elmer Spotlight 400 FTIR imaging system with a germanium ATR crystal. Samples were attached to a glass microscopy slide with cyanoacrylate glue, and data were collected every 50 μm over the insulation thickness of the sample (~ 1.6 mm), with 32 scans per spatial point and a spectral resolution of 1 cm^{-1} . The IR spectra were recorded between 4000 and 750 cm^{-1} and, to quantify the oxidation of the sample, the peak area of the carbonyl band (1720 cm^{-1}) was normalized with respect to the peak area of the methylene asymmetric bending band (1460 cm^{-1}).

2.8. Differential scanning calorimetry

The mass crystallinity (w_c) at 23 $^{\circ}\text{C}$ of the insulation samples were obtained by heating 5 ± 0.5 mg samples from -80 $^{\circ}\text{C}$ to 180 $^{\circ}\text{C}$ at a scanning rate of 10 $^{\circ}\text{C min}^{-1}$ in a Mettler-Toledo differential scanning calorimeter DSC 1. The crystallinity was assessed according to the total enthalpy method [32]:

$$w_c = K \times \left(\frac{\Delta h_{21}}{\Delta h_f^0(T_m^0) - \int_{T_1}^{T_m^0} (C_{p,a} - C_{p,c}) dT} \right) \quad (1)$$

where Δh_{12} is the melting enthalpy obtained by extrapolating the post-melting scanning baseline until it intersected the DSC trace at the low temperature side (at T_1), $\Delta h_f^0(T_m^0)$ is the heat of fusion at the equilibrium melting point (293 J g^{-1}) [33], and $C_{p,a}$ and $C_{p,c}$ are the specific heat capacities of the amorphous and crystalline components, respectively. Data for $C_{p,a}$ and $C_{p,c}$ were obtained from Wunderlich and Baur [34]. The factor K is the ratio of remaining melting at room temperature.

3. Results and discussion

3.1. Dielectric response of unaged and aged cable insulation samples

Figs. 1a and b show the dielectric response for a sample aged for different times at 85 $^{\circ}\text{C}$ and 1.06 kGy h^{-1} expressed as the real and imaginary parts of the dielectric permittivity. With few exceptions, these curves showed an increase over the whole frequency range with increasing ageing time. This increase was most prominent at frequencies below 100 Hz (Figs. 1a and b). Figs. 2a and b display the imaginary part of the dielectric permittivity at 100 kHz (ϵ'' (100 kHz)) plotted as functions of ageing time and irradiation dose, respectively;

ϵ'' (100 kHz) showed a linear increase with increasing ageing time (Fig. 2a). Noteworthy is the split of the data into two different straight lines, depending on the temperature. The irradiation dose dependence of ϵ'' (100 kHz) presented in Fig. 2b show clearly that both the dose rate and the temperature have a significant impact.

Figs. 1a,b and 2a,b

The data for the samples aged at 85 °C showed a dose rate dependence; the imaginary dielectric permittivity increasing with increasing dose rate at a given ageing time (Fig. 2a). The dose rate dependence at a given ageing time implies simply that the dielectric permittivity increased with increasing total dose. The fact that the ageing at the lower temperature (55 °C) was significantly less affected by the dose rate (Fig. 2b) suggests that the process responsible for the change in dielectric loss is limited by oxidation, particularly at the lower ageing temperature. The lower effect of dose rate at lower temperatures has been observed earlier, when ageing at comparably high dose rates [35]. The scatter between repeated measurements was dependent on the frequency, with a greater scatter at lower frequency, approximately 15 % of the absolute value below 1 Hz, and about 1 % at 100 kHz.

3.2. Effect of ageing on the density

The density increased with increasing ageing temperature, increasing irradiation dose and decreasing dose rate (Fig. 3). Differential scanning calorimetry showed that the mass crystallinity of the aged samples was constant and essentially the same as before ageing: 43.9 ± 0.6 % (average \pm standard deviation for samples aged at 55 (0.76 kGy h⁻¹) and 85 °C (0.42 kGy h⁻¹). A linear fit to the experimental data (mass crystallinity versus ageing time) showed a very small increase in crystallinity with increasing ageing time, i.e. from 43.5 % (unaged samples) to 44.4 % (samples aged 1000 h). This change in crystallinity corresponds to an increase in density of 1 kg m⁻³. Thus, the extensive change in density from the initial value of 917 kg m⁻³ to 965 kg m⁻³ (maximum value) must be attributed to oxidation of the amorphous component of the polymer.

Fig. 3

The density of the samples aged at 55 °C showed only moderate dose rate dependence (Fig. 3), and there was a pronounced dose rate dependence on ageing at 85 °C, where the lower dose rate yielded the greater increase in density. These data suggest that the transport of oxygen from the surrounding air into the polymer was important. For a given irradiation dose, the time at the low dose rate (0.42 kGy h⁻¹) was 2.5 times longer than a comparable time at high dose rate (1.06 kGy h⁻¹). The radicals formed due to γ -irradiation were, thus, more prone to react with oxygen and further along the Bolland-Gee oxidation scheme under the low dose rate conditions than at the high dose rates. The smaller change in density for a given irradiation dose of the samples aged at the lower temperature (55 °C) simply reflects that the degree of oxidation of these samples was more moderate due both to slow oxygen diffusion and to a low oxidation rate.

3.3. Changes in the mass fraction of soluble component of the polymer

The mass fraction of the soluble component of the polymer increased with increasing irradiation dose, increasing temperature and decreasing dose rate (Fig. 4). The soluble fraction in the unaged sample was only 16 ± 1 %. The samples aged at 85 °C reached very high values, 40 to 45 %, whereas the samples aged at 55 °C reached only 30 % (Fig. 4). The increase in soluble fraction with irradiation dose was strongest for the samples exposed to the lowest dose rates (Fig. 4). This is consistent with the hypothesis that the oxidation reaction – promoted by a low dose rate – favoured chain scission of the amorphous polymer chains. The lower increase in the samples aged at 55 °C is consistent with the lower increase in density observed in these samples, due to the lower rate of oxidation of the samples at the lower temperature.

Fig. 4

The major effect of the irradiation-induced degradation in the presence of oxygen was, thus, oxidation and scission of amorphous chain segments, which is expected to lead to a lowering of the concentration of tie chains and trapped entanglements, and also of the fracture toughness of the polymer. Exposure of polyethylene to γ -radiation under oxygen-free conditions leads primarily to crosslinking [36]. After oxygen-free γ -irradiation and post-irradiation exposure to oxygen, polyethylene showed a rapid decrease in radical concentration in the amorphous phase by reaction of the amorphous radicals with oxygen, while a much

slower decay of the crystalline radicals enabled slow diffusion of the latter to the crystal/amorphous interface where the reaction between the radicals and oxygen occurred [37,38]. The presence of oxygen during γ -irradiation changes the degradation scenario towards a dominance of scission of the amorphous chains in polyethylene [39–41].

The data for the mass fraction of soluble component presented refer to the entire insulation. It was, however, shown by infrared microscopy that oxidation was macroscopically heterogeneous, being concentrated in the outer parts of the insulation (Section 3.6).

3.5. Mechanical performance

The strain-at-break (ϵ_b) decreased with increasing irradiation dose and decreasing dose rate (Fig. 5). The samples reached a low plateau value after being irradiated by 400 to 600 kGy depending on the dose rate (Fig. 5). The brittle samples, which had reached the low plateau, showed deep surface cracks even prior to the tensile testing. Some of the samples aged under milder conditions also displayed small surface cracks that would provide spots for fracture initiation. Samples exposed to the lowest dose rate (0.42 kGy h⁻¹) showed the strongest decrease in ϵ_b , and they reached the plateau at the lowest irradiation dose (400 kGy).

Fig. 5

The dose rate dependence revealed in Fig. 5 can be explained by the heterogeneous character of the oxidation, as shown by the infrared microscopy data.

3.6. Infrared spectroscopy assessment of polymer oxidation

This section deals with two issues: (i) assessment of the oxidation profiles; (ii) assessment of the average degree of oxidation through the entire insulation. The latter is important in the context of the density data, since it was postulated in Section 3.2 that the significant increase in density in the aged samples was due to oxidation.

The oxidation profiles expressed in terms of carbonyl absorbance normalized with respect to the 1460 cm⁻¹ methylene absorbance of two of the samples studied – one being aged at 55 °C and 1.06 kGy h⁻¹ for 1000 h, and the other at 85 °C and 0.42 kGy h⁻¹ for 600 h – are displayed in Fig. 6. These two samples showed essentially the same overall degree of oxidation considering the entire cross-section. This was confirmed both by integrating the

oxidation profile and by the fact that the samples had the same density values. However, the oxidation profiles were different for the two samples: the sample aged in 1.06 kGy h^{-1} (high dose rate) and $55 \text{ }^{\circ}\text{C}$ (low temperature) showed a very thin layer (thickness = $150 \text{ }\mu\text{m}$) of highly oxidized polymer, whereas the sample aged at 0.42 kGy h^{-1} (low dose rate) and $85 \text{ }^{\circ}\text{C}$ (high temperature) showed a much thicker layer (thickness = $600 \text{ }\mu\text{m}$) of less oxidized polymer. The maximum degree of oxidation was almost 10 times greater in the sample aged at high dose rate and low temperature than in the sample aged at low dose rate and high temperature.

Figs. 6 and 7

It was interesting to note that the sample with the very thin highly oxidized surface skin showed a much lower ϵ_b -value (16 %) than the sample with the considerably thicker oxidized layer (87 %).

The calculation of the average degree of oxidation from the linear carbonyl index profile considered the cylindrical geometry of the insulation: the outer diameter was 2.2 mm and the inner diameter was 0.6 mm . Fig. 7 shows that the calculated average carbonyl index including the entire insulation increased linearly with increasing density. This finding is in accordance with the proposal that oxidation of polyethylene means that hydrogen is partly replaced by carbonyl oxygen; the latter being a heavier element than hydrogen, which is the primary reason for the increase in density on ageing.

3.7. Relationship between electrical and physicochemical properties

The imaginary part of the dielectric permittivity at 100 kHz (ϵ'' (100 kHz)) increased linearly with increasing density (Fig. 8); the latter was confirmed (Section 3.6) to be proportional to the average carbonyl index of the entire insulation. Data obtained for samples aged under different conditions, i.e. different temperatures and different dose rates, fitted well to a straight line, which confirmed that both ϵ'' (100 kHz) and the density were essentially insensitive to the distribution of the oxidized species in the insulation. Thus, the dielectric analytical method can sensitively detect oxidation of the insulation, although it does not provide any information about the oxidation profile through the insulation.

Figs. 8 and 9

Fig. 9 presents the relationship between the strain-at-break and ϵ'' (100 kHz). There is a clear division of the data according to temperature and irradiation dose rate. The samples exposed to a high dose rate at 55 °C suffered highly concentrated oxidation of a thin surface layer, the low strain-at break-plateau being reached at a low ϵ'' (100 kHz), 0.005, whereas samples exposed to a high irradiation dose rate at 85 °C were subjected to more evenly distributed oxidation, the low strain-at break plateau being reached at higher ϵ'' (100 kHz)-value, 0.01.

4. Conclusions

The dielectric response of a cross-linked polyethylene insulation used in nuclear power plants was measured before and after ageing in air at elevated temperatures (55 and 85 °C) and exposure to γ -radiation (0.42, 0.76 and 1.06 kGy h⁻¹) from a ⁶⁰Co-source. These exposures led to polymer oxidation, as revealed directly by infrared spectroscopy and indirectly by a substantial increase in the material density. The material density was proportional to the average carbonyl index of the insulation. Extraction in hot xylene showed that the oxidation of the polymer was accompanied by chain scission of the amorphous component, which was also manifested in a substantial decrease in the strain-at-break of the aged samples. A non-destructive and sensitive dielectric monitoring technique, which assessed the imaginary part of the dielectric permittivity at 100 kHz, yielded data that increased in a strictly linear fashion, independent of the irradiation dose rate, with increasing material density (average carbonyl index). It was shown that the strain-at-break was also very sensitive to the carbonyl index profile through the insulation. Samples consuming oxygen in a very thin surface layer (due to a high irradiation dose rate) showed a greater decrease in strain-at-break than samples irradiated at a lower dose rate with a more uniformly distributed oxidation profile. Since dielectric spectroscopy is a non-destructive technique showing good correlation with the degree of oxidation, it has potential to be used as a condition monitoring technique to follow the oxidation of installed cable insulations to allow for effective ageing management. However, the need for a reference for the output limits its use to shielded cables, and further research is needed to manage the real conditions with junctions, long cables etc. before implementation in nuclear power plants.

Acknowledgements

This study was carried out within the 7th Framework EU Project “Ageing Diagnostics and Prognostics of low-voltage I&C cables” (ADVANCE). Financial support from the European Commission (grant no. 269893) is gratefully acknowledged. Dr. Vit Plaček, ÚJV Řež, a.s., Czech Republic is thanked for providing the aged samples studied.

References

- [1] G. Egusa, J. Mater. Sci. 23 (1988) 2753.
- [2] Assessment and management of ageing of major nuclear power plant components important to safety: in-containment instrumentation and control cables, Volumes I and II; December, 2000. IAEA-TECDOC-1188.
- [3] K.T. Gillen, R.L. Clough, (SAND-90-2009) Energy Res. Abstr. 16 (1991) 3.
- [4] Y. Ohki Y, IEEE Trans. Electr. Insul. 21 (1986) 919.
- [5] R.L. Clough, K.T. Gillen, Polym. Mater. Sci. Eng. 52 (1985) 592.
- [6] K.T. Gillen, M. Celina, R.L. Clough, Trends Polym. Sci. 5 (1997) 250.
- [7] J. Wise, K.T. Gillen, R.L. Clough, Radiat. Phys. Chem. 49 (1997) 565.
- [8] V. Plaček, B. Bartoniček, V. Hnát, B. Otáhal, Nucl. Instr. Meth. Phys. Res. B 208 (2003) 448.
- [9] Pilot study on the management of ageing of instrumentation and control cables; March, 1997. IAEA-TECDOC-932.
- [10] K.T. Gillen, M. Celina, R.L. Clough, Radiat. Phys. Chem. 56 (1999) 429.
- [11] J.V. Gasa, Z. Liu Z, M.T. Shaw, Polym. Degrad. Stab. 87 (2005) 77.
- [12] B. Bartoniček, V. Hnát, V. Plaček, Radiat. Phys. Chem. 52 (1998) 639.
- [13] K. Anandakumaran, W. Seidl, P.V. Castaldo, IEEE Trans. Dielectr. Electr. Insul. 6 (1999) 376.
- [14] L.R. Mason, T.E. Doyle, A.B. Reynolds, J. Appl. Polym. Sci. 50 (1993) 1493.

- [15] K.T. Gillen, R. Bernstein, R.L. Clough, M. Celina, *Polym. Degrad. Stab.* 91 (2006) 2146.
- [16] K.T. Gillen, R.A. Assink, R. Bernstein, *Polym. Degrad. Stab.* 84 (2004) 419.
- [17] T. Seguchi, K. Tamura, T. Ohshima, A. Shimada, H. Kudoh, *Radiat. Phys. Chem.* 80 (2011) 268.
- [18] R.L. Clough, K.T. Gillen, *Radiat. Phys. Chem.* 18 (1981) 661.
- [19] M. Ekelund, P.F. Fantoni, U.W. Gedde, *Polym. Testing* 30 (2011) 86.
- [20] Z.Á. Tamus, I. Berta, *Proc. IEEE EIC Montreal, Canada* (2009) 444.
- [21] J.M. Braun, *IEEE Electr. Insul. Mag.* 8(5) (1992) 27.
- [22] L. Verardi, D. Fabiani, G.C. Montanari, *Radiat. Phys. Chem.* 94 (2014) 166.
- [23] C. Lee, K.B. Lee, *J. Ind. Eng. Chem.* 14 (2008) 473.
- [24] J.F. Chailan, G. Boiteux, J. Chauchard, B. Pinel, G. Seytre, *Polym. Degrad. Stab.* 47 (1995) 397.
- [25] C.S. Shah, M. J. Patni, M.V. Pandya, *J. Mater. Sci.* 32 (1997) 6119.
- [26] F.I. Mopsik, F.D. Martzloff, *Nucl. Eng. Des.* 118 (1990) 505.
- [27] J.F. Chailan, G. Boiteux, J. Chauchard, B. Pinel, G. Seytre, *Polym. Degrad. Stab.* 48 (1995) 61.
- [28] J. Viard, *J. Appl. Phys.* 73 (1993) 890.
- [29] P.C.N. Scarpa, A.T. Bulinski, S. Bamji, D.K. Das-Gupta, *IEEE Conference on Electrical Insulation and Dielectric Phenomena Annual Report 1994*, 437.
- [28] P. Werelius, P. Thärning, R. Eriksson, B. Holmgren, U. Gäfvert, *IEEE Trans. Dielectr. Electr. Insul.* 8 (2001) 27.
- [31] A.B. Reynolds, R.M. Bell, N.M.N. Bryson, T.E. Doyle, M.B. Hall, L.R. Mason, L. Quintric, P.L. Terwilliger, *Radiat. Phys. Chem.* 45 (1995) 103.
- [32] A.P. Gray, *Thermochim. Acta* 1 (1970) 563.
- [33] B. Wunderlich, *Macromolecular Physics, Vol 3: Crystal Melting*, Academic Press, New York, 1980.
- [34] B. Wunderlich, H. Baur, *Adv. Polym. Sci.* 7 (1970) 151.

- [35] Assessing and Managing Cable Ageing in Nuclear Power Plants; May, 2012. IAEA Nuclear Energy Series NP-T, Annex A2.5.
- [36] A. Charlesby, Irradiation Effects on Polymers, eds. D.W. Clegg, A.A. Collyer, Chapter 2: The effects of ionizing radiation on polymers, Elsevier Applied Science, London and New York, p. 39, 1991.
- [37] B.R. Loy, J. Polym. Sci. 44 (1966) 341.
- [38] M. Dole, G.G.A. Bohm, Radiation Research 1966, North Holland, Amsterdam, 1967.
- [39] K. Arakawa, T. Seguchi, Y. Watanabe, N. Hayakawa, J. Polym. Sci, Polym. Chem. Ed. 20 (1982) 2681.
- [40] D.J. Carlsson, G. Bazan, S. Chmela, D.M. Wiles, Polym. Degrad. Stab. 19 (1987) 195.
- [41] L. Costa, M.P. Luda, L. Trussarelli, E.M. Brach del Prever, M. Crova, P. Gallinaro, Biomaterials 19 (1998) 659.

Legends to Figures

Fig. 1a. The real part of the dielectric permittivity (ϵ') plotted as a function of the frequency (logarithmic scale) for unaged and aged samples after exposure to 1.06 kGy h⁻¹ irradiation at 85 °C in air.

Fig. 1b. The imaginary part of the dielectric permittivity (ϵ'' ; logarithmic scale) plotted as a function of the frequency (logarithmic scale) for unaged and aged samples after exposure to 1.06 kGy h⁻¹ irradiation at 85 °C in air.

Fig. 2a. Imaginary part of the dielectric permittivity at 100 kHz (ϵ'' (100 kHz)) plotted as a function of ageing time for samples aged in air under different combinations of temperature and irradiation dose rate.

Fig. 2b. Imaginary part of the dielectric permittivity at 100 kHz (ϵ'' (100 kHz)) plotted as a function of irradiation dose for samples aged in air under different combinations of temperature and irradiation dose rate.

Fig. 3. Density of unaged and aged samples aged in air using different combinations of temperature and irradiation dose rate plotted as a function of irradiation dose.

Fig. 4. The mass fraction of soluble component in unaged and aged samples aged in air using different combinations of temperature and irradiation dose rate plotted as a function of irradiation dose.

Fig. 5. The strain-at-break (ϵ_b) of unaged and aged samples aged in air using different combinations of temperature and irradiation dose rate plotted as a function of irradiation dose.

Fig. 6. Carbonyl index (area of the carbonyl band at 1720 cm⁻¹ divided by the area of the methylene band at 2850 cm⁻¹) plotted as a function of distance from the outer surface of the insulation for samples aged in air at 85 °C and 0.42 kGy/h, for 600 h (filled circles, line a) and 55 °C and 1.06 kGy/h for 1000 h (open circles, line b).

Fig. 7. Average carbonyl index for entire insulation plotted as a function of the density of the materials. The straight line is a linear fit to the experimental data. The point marked with an arrow is an outlier; this sample displayed deep surface cracks.

Fig. 8. The imaginary part of the dielectric permittivity at 100 kHz (ϵ'' (100 kHz)) plotted as a function of density of unaged and aged samples aged in air using different combinations of temperature and irradiation dose rate.

Fig. 9. The strain-at-break (ϵ_b) plotted as a function of the imaginary part of the dielectric permittivity at 100 kHz (ϵ'' (100 kHz)) for unaged and aged samples aged in air using different combinations of temperature and irradiation dose rate.

ACCEPTED MANUSCRIPT

